Title
Molecular cloning and characterization of three human cellular proteins that interact with the HIV-1 nef protein

Author
Hsue, Priscilla,

Publication Date
1996

Peer reviewed|Thesis/dissertation

Molecular Cloning and Characterization of Three Human Cellular Proteins That Interact with the HIV-1 Nef Protein

by

Priscilla Hsue

Abstract

The human immunodeficiency virus type 1(HIV-1) is a pathogenic lentivirus that contains nine distinct genes. One of these genes termed *nef* has been shown to be required for the production of high viral burdens and clinical development of AIDS. The 27-30 kD Nef protein exerts two principal known biologic effects -- enhancement of viral infectivity and down-regulation of surface CD4, the principal high affinity receptor for HIV.

To further understand the molecular basis for these dual functions of Nef, we have employed the yeast two-hybrid assay of protein-protein interaction to identify three cellular cDNAs encoding **N**ef **A**ssociating **P**roteins (NAPS 1,2,and 3). Each of these NAPs appears to be ubiquitously expressed in human tissues based on mRNA analysis.

Further study revealed that NAP1 and NAP3 form homodimers while NAP2 forms heterodimers with both NAP1 and NAP3. Additionally, the binding of NAP1 but not NAP2 or NAP3 to Nef was inhibited by mutation of a SH3-like (proline-rich) binding motif within Nef that concommitantly disrupted Nef-mediated enhancement of viral infectivity.

The second major function of Nef, CD4 downregulation, appears to represent a 2-step process. First, $p56^{lck}$, a src-like tyrosine kinase, must be removed from the cytoplasmic tail of CD4 followed subsequently by endocytosis of CD4 via clathrin coated pits. However, Nef does not appear to bind directly to either $p56^{lck}$ or the CD4 cytoplasmic tail. We have found that NAP2 physically binds not only to Nef but also to $p56^{lck}$. Thus, NAP2 may either bridge Nef and $p56^{lck}$ or alternatively, Nef may compete NAP2 away from $p56^{lck}$. In each case, the Nef-NAP2 interaction may be important in the initial clearance of $p56^{lck}$ from the CD4 tail. Additional characterization of

these NAPS using specific anti-NAP antibodies and full-length NAP expression vectors should permit further dissection of the molecular basis for Nef action. In view of the requirement of Nef for disease production, these Nef-NAP interactions may represent attractive new targets for anti-viral drug design.

Table of Contents:

Abstract	ii
List of Tables	v
List of Figures	vi
Introduction	1
Methods	2
Results	5
Discussion	8
Bibliography	12
Acknowledgments	15
Tables	16
Figures	21

List of Tables:

Table 1, page 16: cDNA and mRNA Sizes for NAPs 1,2, and 3

Table 2, page 17: Quantitative ß-galactosidase assay demonstrating the relative avidity of NAPS for Nef

Table 3, page 18 Homo-and Hetero-oligomerization of NAPs in the Yeast Two-Hybrid System

Table 4, page 19: Summary of Mapping of Nef and NAPs

Table 5, page 20: The $(Pxx)_4$ /Putative PKC Phosphorylation Site of Nef Is Important for Both NAP1 Binding and Infectivity

List of Figures

Figure 1, page 21: HIV-1 Virion Structure and Genomic Organization

Figure 2, page 22: The HIV-1 Receptor: CD4-p56^{lck} Complex

Figure 3, page 23: Yeast Two-Hybrid Assay of Protein-Protein Interaction

Figure 4, page 24: Effector plasmids utilized in the two-hybrid system

Figure 5, page 25: HeLa cDNA library screen using a Nef-Gal4 DNA binding domain fusion protein (pGBNef)

Figure 6, page 26: Nef and NAP Interactions

Figure 7, page 27: NAP mRNA Species and Tissue Distribution

Figure 8, page 28: NAP2-Interacts with Both Nef and p56^{lck}

Figure 9A, B, pages 29, 30: Deletion Analysis of NAP2

Figure 10, page 31: Model 1 - Distinct NAP2 Binding Sites

Figure 12, page 32: Model 2 - Overlapping NAP2 Binding Sites

Figure 13, page 33: NAP2 Binds Directly to the SH3 Domain of p56^{lck}

Introduction:

The human immunodeficiency virus (HIV) has spread rapidly since its detection in 1981, with estimates of over 22 million individuals currently infected (1). As antiviral therapy remains limited, the need to develop new therapeutic approaches has increased dramatically. One method for facilitating the development of the next generation of effective anti-viral therapies involves discerning the molecular basis for HIV pathogenesis. HIV is the prototypical human member of the lentivirus family and is remarkable for its genetic complexity (Fig. 1). In addition to the *gag*, *pol*, and *env* genes found in all replication competent retroviruses, HIV encodes at least six additional regulatory proteins (2). The proteins encoded by the *nef*, *tat*, and *rev* genes are expressed early in the viral life cycle while the proteins encoded by the *vif*, *vpu*, and *vpr* genes are expressed later in the viral life cycle.

Our laboratory has chosen to focus on the HIV *nef* gene product. The 27-30 kD Nef protein is conserved in primate lentiviruses suggesting that it serves an important function. Early studies demonstrated a negative effect of Nef on transcriptional activity of the HIV-1 LTR and viral growth, hence the acronym for negative factor (3,4). However, an experiment in adult rhesus macaques using an SIV variant defective in the *nef* gene revealed that this viral regulatory protein is critical for the maintenance of high viral burdens and the development of AIDS (5). Interestingly, in this same model, SIV with a *nef* deletion has served as an effective, live attenuated vaccine (6). Subsequent in vitro studies confirmed that Nef actually functions as a positive factor serving to enhance the rate of viral replication in culture (7,8,9).

Another known function of Nef involves down-regulation of surface

CD4 (10,11,12). The CD4 receptor is the primary high affinity receptor for HIV, and its removal by Nef from the cell surface is thought to occur in two steps (Fig. 2). First, $p56^{lck}$, a member of the Src family of tyrosine kinases, dissociates from the cytoplasmic tail of CD4 (13, 14). The CD4 molecule is then endocytosed via clathrin coated pits and degraded in lysosomes. Although Nef mediates this process, it does not appear to bind directly to CD4, implying that one or more cellular cofactors are likely to be involved.

Finally, a recent study has identified an HIV-positive blood donor and recipients who have all remained free of disease for more than 10 years (15). When characterized further, it was found that all of these patients had been infected with viruses from a single donor that contained a deletion in the *nef* gene. This study further emphasizes the pivotal role of Nef in determining HIV-1 pathogenesis.

We hypothesized that Nef mediates its effects by interacting with cellular proteins. Recent biochemical data has demonstrated an association between Nef and two proteins of 62kD and 72kD that are phosphorylated in vitro (16), but the identify and function of these phosphoproteins are not yet known. We employed the yeast two-hybrid system of identifying protein-protein interactions to identify and characterize proteins that physically interact with Nef in order to further dissect the molecular basis of Nef action.

Methods:

The yeast two-hybrid assay was used to identify proteins that interact with Nef. This assay has been described previously (17) and makes use of the modular properties of the yeast GAL4 transcription factor which can be

dissected into a DNA binding domain and a transcriptional activation domain. DNA encoding a particular protein of interest is fused to the GAL4 DNA binding domain while DNA encoding another protein (a potential partner) or a library of proteins can be fused to the GAL4 activation domain (Fig. 3). We have used a plasmid which contains the DNA binding domain fused to a selectable *trp* marker (pGBT9) which enables yeast to grow in the absence of the amino acid tryptophan and a plasmid containing the GAL4 activation domain fused to a *leu* marker(pGAD424) which permits yeast to grow in the absence of leucine (Fig.4). The two plasmids are co-transformed into yeast and then grown on selective media deficient in tryptophan and leucine. If the proteins of interest physically interact, then the two domains of the GAL4 transcription factor will be juxtaposed, and transcriptional activation of a downstream reporter gene will occur. We have used two types of reporters in our two-hybrid screen. The first is a GAL4 responsive His marker which permits yeast to grow in the absence of histidine. The second is ß-galactosidase which allows interacting proteins to be detected by a blue color change when the chromogenic substrate X-gal is added.

In the first part of the study, the *nef* gene was fused in frame to the GAL4 DNA binding domain in the yeast pGBT9 vector. A HeLa cDNA library inserted into a pGAD424-like vector and was screened with the GAL4-Nef fusion. These vectors were co-transformed into yeast and then assayed for both growth in the absence of histidine and ß-galactosidase activity. His^{+}ß-gal^{+} clones were isolated, tested for Nef specificity, and sequenced (Fig. 5). The level of transcription activation was quantified using a liquid ß-gal assay (18).

Yeast colonies were picked and grown in selective liquid media overnight. Yeast were then lysed, and ONPG was used as a substrate for the ß-gal reaction. ß-gal units are calculated using the following reaction:

ß-gal units = 1000 x OD 420 / (t x V x OD600)

where t= time in min of incubation, V= 0.1ml x concentration factor, and OD600 = abs at 600nm of 1 ml of culture

Northern blot analyses were performed using nitrocellulose filters containing polyA mRNA from various human tissues. NAP1, 2, and 3 cDNAs were radiolabeled with ^{32}P and used as probes to study the tissue distribution of the NAPs.

Protein expression was also analyzed using Western blot analyses. Yeast cultures were grown overnight in selective media and lysed in SDS-containing sample buffer using glass beads. The lysates were subjected to SDS-PAGE. After transfer to nitrocellulose filters, the samples were incubated with a primary anti-GAL4 DNA binding domain antibody (at a dilution of 1:1000) and then incubated with a secondary antibody conjugated to HRP. An HRP substrate was added and proteins were visualized using enhanced chemiluminescent detection.

In the second portion of the study, NAP-NAP interactions were tested in the yeast two-hybrid assay. NAPs 1, 2, and 3 were subcloned into the pGBT9 vector and tested with NAPs 1, 2, and 3 in the pGAD424 vector obtained from the library screen. The plasmids were co-transformed into yeast and then assayed for ß-gal activity.

A series of point mutants in conserved regions of Nef(19) were constructed and then tested for their ability to bind to the NAPs in the two-hybrid assay and in functional assays for viral infectivity and CD4

downregulation. The MAGI assay (20) was used to measure viral infectivity. In brief, this assay employs a HeLa cell line engineered to express CD4, permitting HIV infection. In addition, these cells contain a ß-galactosidase gene placed under control of the HIV-1 LTR. As such, viral infection leads to the production of HIV Tat which drives transcription of the reporter gene, resulting in a blue color change which can be visualized using light microscopy.

For the CD4 down-regulation assay, COS cells were co-transfected with combinations of CD4 and Nef and compared with cells transfected with CD4 alone. CD4 expression was detected using a fluorescent anti-CD4 antibody and analyzed on a Becton Dickinson FACScan.

In the final portion of the study, the ability of CD4 and $p56^{lck}$ to bind to the NAPs was assayed using the two-hybrid system. A series of deletion mutants of NAP2 was constructed and tested for their ability to bind to Nef, $p56^{lck}$, and NAP3. Finally, a series of deletion mutants of $p56^{lck}$ was constructed and tested for their capacity to bind NAP2.

Results:

The HeLa cDNA library screen resulted in the molecular cloning of three distinct cellular cDNAs that encode proteins that specifically interact with the HIV-1 *nef* gene product in the yeast two-hybrid system. Each of these proteins failed to react with a series of control proteins including HIV Gag, Vif, Vpu, gp41 tail, lamin, and CD4 tail, indicating a specific interaction with Nef. We have termed these proteins **N**ef **A**ssociating **P**roteins -- NAP1, NAP2, and NAP3 (Fig. 6). The cDNA sizes for NAPs 1,2, and 3 were 1216 bp, 1074 bp, and 1223 bp, respectively (Table 1). A Genbank search revealed that

each of these sequences was unique and have not been previously identified. The quantitative liquid ß-galactosidase assay demonstrated that NAP1 had the strongest apparent avidity for Nef (926 B-gal units), the Nef-NAP2 pair had an intermediate apparent avidity (82 B-gal units), while the Nef-NAP3 pair had the weakest apparent avidity (26 B-gal units) (Table 2). Northern blot analyses revealed that the three NAPs were expressed in all human tissues tested (Fig. 7). Interestingly, the pattern of distribution differed, with NAP1 and NAP3 being most highly expressed in skeletal muscle while NAP2 was most highly expressed in skeletal muscle and spleen. The mRNAs obtained for NAPs 1,2,3 were 3000 bp, 4400bp, and 1350 bp, respectively (Table 1).

Assays for NAP-NAP interactions showed that both NAP1 and NAP3 homodimerize. In addition, both NAP1 and NAP3 formed heterodimers with NAP2. NAP1 failed to interact with NAP3. The liquid ß-galactosidase assay showed that the NAP1-NAP1 homodimer had the strongest interaction along with the NAP2-NAP3 heterodimer (Table 3). The NAP3-NAP3 homodimer was intermediate in strength while the NAP1-NAP2 interaction was the weakest.

A series of Nef mutants was next analyzed for their ability to bind to the NAPs (Table 4) . The Nef G2A point mutant is located in the myristylation signal sequence of Nef and was found to have no effect on the ability of the NAPs to bind to Nef. We found that the Nef $(Pxx)_4$ mutant which mutates all four prolines in a proline-rich region of Nef needed for viral infectivity was completely unable to bind to NAP1, suggesting that the proline residues of Nef are critical for Nef-NAP1 association. In contrast, this mutant was still able to bind NAPs 2 and 3, suggesting that they bind to other

regions of Nef. The Nef T80A point mutant alters a putative site for phosphorylation by protein kinase C. This mutant was found to have a weakened ability to bind to NAP1 but normal binding to NAP2 and NAP3. Expression of each of the mutants was confirmed in Western blot analysis using an antibody against the GAL4 DNA binding domain.

The viral infectivity assay showed the Nef G2A point mutant was most severely impaired in its ability to rescue infectivity (8% activity of wild type Nef) (Table 5). The Nef $(Pxx)_4$ mutant had an intermediate infectivity level at 14%. The Nef T80A point mutant had the greatest ability of the mutants tested to rescue viral infectivity with a level of 34%. For the CD4 down-regulation assay, again the Nef G2A was found to be most impaired of the mutants with a level of 20% of the control. Both the Nef (Pxx)4 mutant and Nef T80A point mutant were only mildly affected in their ability to down-regulate CD4 from the cell surface with levels of 80% and 87% respectively.

Using the two-hybrid assay, we found that NAP2 not only binds to Nef but also binds to $p56^{lck}$ (Fig. 8). In contrast, NAP 2 failed to bind to the cytoplasmic tail of CD4, and both NAP1 and NAP3 did not interact with either $p56^{lck}$ or the CD4 tail. Deletion mutant analysis of NAP2 showed that both Nef and $p56^{lck}$ bind to the same general overlapping region of NAP2 (Fig. 9A, Fig. 9B), namely amino acids 30 to 131. Interestingly, NAP3 required a larger region of NAP2 for binding, spanning amino acids 1-161. Deletion mutants of $p56^{lck}$ suggest that the SH3 domain alone of this tyrosine kinase is sufficient for binding to NAP2. NAP2 was also found to interact weakly with Fyn while failing to bind to Hck, two other members of the Src family.

Discussion:

Studies of the HIV-1 Nef protein have revealed that it exerts two principal biologic effects -- enhancement of viral infectivity and down-regulation of surface CD4. To better understand the molecular basis for these dual functions of Nef, we pursued the identification of cellular proteins that physically associate with Nef. For these studies, we have employed the yeast two-hybrid assay of protein-protein interactions. This approach has permitted the molecular cloning of three distinct cellular cDNAs that encode proteins that specifically interact with the HIV-1 *nef* gene product. These proteins have been termed Nef Associating Proteins -- NAP1, NAP2, and NAP3.

NAP1 was the strongest inducer of transcription in conjunction with Nef while NAP3 was the weakest inducer in the two-hybrid assay. In addition to interacting with Nef, our analyses demonstrate that the NAPs interact amongst themselves with differing avidities. This data on protein-protein interactions suggests that the Nef-NAP interactions may occur in multimolecular complexes, possibly involving more than one NAP. We are currently in the process of demonstrating these Nef-NAP interactions in mammalian cells.

Analysis of the Nef mutants in the two-hybrid assay combined with the functional assays for viral infectivity and CD4 down-regulation permits delineation of certain structure-function relationships. For example, the Nef G2A mutant was impaired in both the assays of viral infectivity and CD4 down-regulation, presumably because this mutant is unable to localize to the membrane. Our analysis revealed that mutation of the proline-rich region in Nef inhibited binding to NAP1 but had no effect on the binding of NAP2 or NAP3. This same mutant, the Nef $(Pxx)_4$ mutant, which is completely

unable to bind NAP1, was found to be severely impaired in its ability to rescue viral infectivity while maintaining its ability to down-regulate CD4. Similarly, the Nef T80A mutant which had a weakened yet not completely abolished ability to bind NAP1, displayed a greater ability to rescue viral infectivity than the Nef $(Pxx)_4$ mutant. The Nef T80A mutant, similar to the Nef$(Pxx)_4$ mutant, was only mildly impaired in the CD4 down-regulation assay. We hypothesize that NAP1 may play a role in Nef-induced enhancement of viral infectivity. The specific mechanism of how Nef acts to enhance viral infectivity remains unclear, with its effect most likely exerted at a point distal to virion uptake (21). Our results suggest that NAP1 or a multimolecular complex that includes NAP1 interacts with Nef via its proline residues to assist Nef at some point during the infection process.

We have found that NAP2 binds not only directly to Nef but also to $p56^{lck}$. As previously noted, Nef promotes the down-regulation of CD4 which requires the initial removal of $p56^{lck}$ in cells expressing this tyrosine kinase, followed by the endocytosis and degradation of CD4. Our findings suggest that NAP2 may serve as a cellular bridge to link both Nef and $p56^{lck}$ or alternatively, Nef may compete NAP2 away from $p56^{lck}$. With this interaction in mind, there are two possible models to explain the data. In the first model (bridge model), NAP2 has distinct binding sites for both Nef and $p56^{lck}$ (Fig. 10). A second model (competition model) involves overlapping binding sites on NAP2 for both Nef and $p56^{lck}$ (Fig.11). In this model, NAP2 serves to stabilize the $p56^{lck}$-CD4 complex in the absence of Nef. However, in the presence of Nef, NAP2 binding to $p56^{lck}$ is blocked, causing $p56^{lck}$ to dissociate, and then CD4 to become internalized. Analysis of various

deletion mutants indicates that both Nef and $p56^{lck}$ bind to the same general region of NAP2, providing some support for the second model of a competitive interaction.

Members of the Src tyrosine kinase family have regions of homology termed SH3 and SH2 domains in addition to their amino terminal unique domains and carboxy terminal catalytic and regulatory domains. A minimal PxxP consensus motif has been identified which is involved in binding to the SH3 domains (22, 23). We found that the SH3 domain alone of $p56^{lck}$ is sufficient for binding to NAP2 (Fig. 12). Inspection of the region in NAP2 (amino acids 30 to 131) that is necessary for binding to $p56^{lck}$ shows that it contains a PxxPxxP motif which resembles the previously identified PxxP SH3 binding motif. We hypothesize that the proline residues located in the $p56^{lck}$ binding region of NAP2 may mediate binding to the SH3 domain of $p56^{lck}$. Experiments involving mutagenesis of these proline residues are underway to confirm this hypothesis. In addition, we have found that NAP2 can bind to another member of the Src family of tyrosine kinases, namely Fyn, but fails to interact with Hck demonstrating a certain degree of specificity. The nature of these interactions remains to be defined, particularly whether SH3 domains are involved.

Additional characterization of these NAPS using specific anti-NAP antibodies and full length NAP expression vectors should permit further dissection of the molecular basis for Nef action. We are currently in the process of confirming physical interaction of Nef and the NAPs in mammalian cells, preparing specific anti-NAP antibodies, and isolating full-length cDNAs for NAPs 1,2, and 3. In the future, we plan to perform analysis of the functional effects of the NAPs in order to better understand the

character of their interaction with Nef and in turn how they promote Nef function. In light of the requirement of Nef for disease progression, it remains possible that further analysis of Nef-NAP interactions may provide attractive new targets for the future design of novel anti-viral therapies.

Bibliography:

1. Greene, W.C. AIDS and the immune system. *Scientific American*, 1993. 269:98-105.

2. Greene, W.C. The molecular biology of human immnodeficiency virius type 1 infection. *N Engl J Med*, 1991. 324:308-317.

3. Niederman, T.M. J., B. Thielan and L. Ratner. Human immunodeficiency virus type 1 negative factor is a transcriptional silencer. *Proc Natl Acd Sci USA*, 1989. 86: 1128-32.

4. Ahmad, N. and S. Venkatsan. Nef protein of HIV-1 is a transcriptional repressor of HIV-1LTR. *Science*. 241: 1481-5.

5. Kestler, H.W., III, D.J. Ringler, K. Mori, D.L. Panicali, P.K. Sehgal, M.D. Daniel and R.C. Desrosiers. Importance of the nef gene for maintenance of high virus loads and for development of AIDS. *Cell*, 1991. 65:651-652.

6. Daniel, M.D., F. Kirchhoff, S.C. Czajak, et al. Protective effects of a live attenated SIV vaccine with a deletion in the nef gene. *Science*, 1992. 258:1938-41.

7. Hammes, S. R., E.P. Dixon, M.H. Malim, et al. Nef protein of human immunodeficiency virus type 1: evidence against its role as a transcriptional inhibitor. *Proc Natl Acad Sci USA*, 1989. 86: 9549-53.

8. Kim, S., K. Ikeuchi, R. Byrn, et al. Lack of a negative influence on viral growth by the nef gene of human immunodeficiency virus type 1. *Proc Natl Acad Sci USA*, 1989. 86:9544-8.

9. Miller, M.D., M.T., Warmerdam, I. Gaston, W.C., Greene and M.B. Feinberg. The human immunodeficiency virus-1 nef gene product: a positive factor for viral infection and replication in primary lymphocytes and

macrophages. *J Exp Med*, 1994. 179:101-113.

10. Garcia, J. V. and A.D. Miller. Serine phosphorylation-independent downregulation of cell-surface CD4 by nef. *Nature*, 1991. 350: 508-11.

11. Garcia, J.V., J. Alfano and A.D. Miller. The negative effect of human immunodeficiency virus type 1 Nef on cell surface CD4 expression is not species specific and requires the cytoplasmic domain of CD4. *J Virol*, 1993. 67: 1511-6.

12. Mariani, R., and J. Skowronski. CD4 downregulation by nef alleles isolated from human immunodeficiency virus type 1 infected individuals. *Proc Natl Acad Sci USA*, 1993. 90: 5549-5553.

13. Haughn, L., S. Gratton, L. Caron, et al. Association of tyrosine kinase $p56^{lck}$ with CD4 inhibits the induction of growth through the alpha beta T-cell receptor. *Nature*, 1992. 358: 328-31.

14. Sleckman, B.P., J. Shin, V.E. Igras, et al. Disruption of the CD4-$p56^{lck}$ complex is required for rapid internalization of CD4. *Proc Natl Acad Sci USA*, 1992. 89: 7566-7570.

15. Deacon, N.J., A. Tsykin, A. Solomon, et al. Genomic Structure of an Attenuated Quasi Species of HIV-1 from a Blood Transfusion Donor and Recipients. *Science*, 1995. 270: 988-991.

16. Sawai, E.T., A. Baur, H. Struble, B.M. Peterlin, J.A. Levy and C. Cheng-Mayer. Human immunodeficiency virus type 1 Nef associates with a cellular serine kinase in T lymphocytes. *Proc Natl Acad Sci USA*, 1994. 91: 1539-1543.

17. Fields, S. and O. Song. A novel genetic system to detect protein-protein interactions. *Nature*, 1989. 340: 245-6.

18. Clontech Matchmaker Two-Hybrid Product Protocol.

19. Shugars, D.C. M.S. Smith, D.H. Glueck, P.V. Nantemet, F.Seillier-Moiseiwitsch and R. Swanstrom. Analysis of human immunodeficiency virus type 1 nef gene sequences in vivo. *J Virol*, 1993. 67: 4639-4650.

20. Kimpton, J., and M. Emerman. Detection of replication-competent and pseudotyped HIV with a sensitive cell line on the basis of acivation of an integrated ß-galactosidase gene. *J. Virol.*, 1992. 66: 2232-2239.

21. Miller, M.D., M. T. Warmerdam, K.A. Page, et al. Expression of the human immunodeficiency virus type 1 (HIV-1) *nef* gene during HIV-1 production increases progeny particle infectivity independent of gp160 or viral entry. *J. Virol.*, 1995. 69: 579-584.

22. Mayer, B.J., and D. Baltimore. Signalling through SH2 and SH3 domains. *Trends Cell Biol*, 1993. 3:8-13.

23. Pawson, T. and J. Schlessinger. SH2 and SH3 domains. *Current Biology*, 1993. 3: 434-442.

Acknowledgments:

This project was funded by the Research Training Fellowship for Medical Students program from the Howard Hughes Medical Institute. I would like to thank Dr. Warner C. Greene for giving me the chance to work in his laboratory and all his support, Dr. Romas Geleziunas for his tremendous teaching and support, and Dr. Diane Colby and Dr. Anthony DeFranco for their critical review of this manuscript.

Table 1
cDNA and mRNA Sizes for NAPs 1,2, and 3

The NAP cDNA sizes obtained from the Hela cDNA library screen are shown. The mRNA sizes for the NAPs obtained from Northern blot analyses are listed along with the sizes of the missing cDNA portions.

	NAP1	NAP2	NAP3
cDNA size (bp)	1216	1074	1223
mRNA size (bp)	3000	4400	1350
missing from cDNA (bp)	1784	3326	127

Table 2
Quantitative ß-Galactosidase Assay Demonstrating the Relative Avidity of NAPs for Nef

Colonies resulting from the yeast co-transformation are assayed using plate lifts and liquid cultures. For the plate lifts, colonies are lifted onto nitrocellulose filters, soaked in an X-gal substrate, and incubated at 30 ^{o} C. The resulting blue colonies can then be observed. For the liquid assay, colonies are picked, grown overnight in selective media, and lysed. An ONPG substrate is added, and the resulting color change is measured using a spectophotometer. ß-gal units are calculated using the following formula: ß-gal units = 1000 x OD420/ (t x V x OD600) where t = time in minutes of incubation, V = 0.1ml x concentration factor, and OD600 = Abs at 600nm of 1ml of culture.

Plasmids	Plate lift/ β–Galactosidase assay	Liquid β-Galactosidase assay (β-gal units x 10^{-1})
pGBNef+pGAD424	white	3
pGBT9+pNAP1	white	2
pGBNef+pNAP1	blue	926
pGBT9+pNAP2	white	3
pGBNef+pNAP2	blue	82
pGBT9+pNAP3	white	2
pGBNef+pNAP3	light blue	26
p53+Tag	blue	273

Table 3
Homo and Hetero-oligomerization of the NAPs in the Two-Hybrid System

The NAPs were tested in the two-hybrid assay to determine if they could interact amongst each other. ß-gal units ($x10^{-1}$) were calculated as previously described. N.D. = no data could be obtained for NAP2 as it was found to have a background level of transcriptional activity.

		Gal4 Activation Domain Fusion		
		NAP1	**NAP2**	**NAP3**
Gal4 DNA Binding Domain Fusion	**NAP1**	**875**	**34**	**0**
	NAP2	**N.D.**	**N.D.**	**N.D.**
	NAP3	**0**	**956**	**186**

Table 4
Summary of Mapping of Nef and NAPs

Mutations in conserved regions of Nef were tested for their binding ability to the NAPs. The NefG2A mutant mutates a glycine residue located in the myristylation signal sequence of Nef to an alanine. The Nef(Pxx)4 mutant mutates all four prolines in a proline-rich region of Nef to alanines. The Nef T80A mutates a threonine residue which is located in a putative site of phosphorylation by protein kinase C to alanine . The expression of each of the Nef mutants was verified using Western blot analysis. The symbol + indicates a blue color change in the ß-gal assay, +/- indicates a light blue color change, and - indicates no color change.

Nef mutants	**NAP1**	**NAP2**	**NAP3**	**Expression**
Nef	+	+	+	+
Point Mutations				
Nef G2A	+	+	+	+
Nef $(Pxx)_4A$	-	+	+	+
Nef T80A	+/-	+	+	+

Table 5
The (Pxx)4/Putative PKC Phosphorylation Site of Nef Is Important for Both NAP1 Binding and Infectivity

Structure-function analysis of the ability of the Nef mutants to bind to NAP1 and their function in assays for viral infectivity and CD4 down-regulation are shown. The MAGI assay (20) developed by Kimpton and Emerman was used for the viral infectivity assays. For the CD4 down-regulation assay, COS cells were cotransfected with combinations of CD4 and Nef and compared with cells transfected with CD4 alone. For both of the functional assays, the ability of wild type Nef to enhance viral infectivity or down-regulate CD4 was assigned a value of 100%.

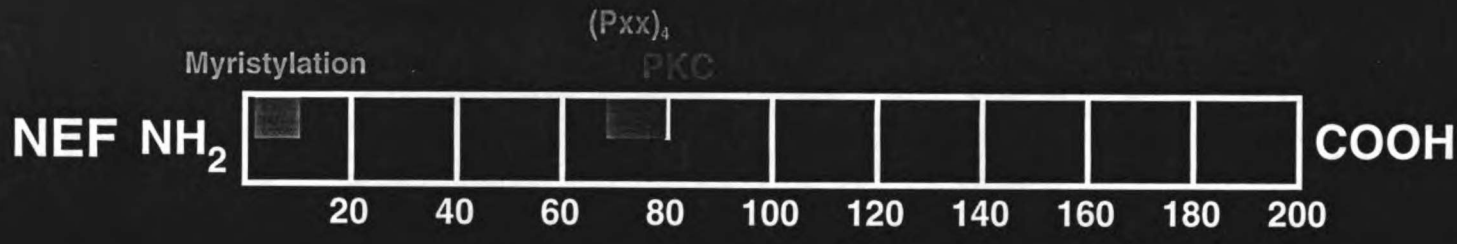

	NAP1 Binding	Viral Infectivity (% of Control)	CD4 Down-regulation (% of Control)
Nef	+	100	100
Nef Mutants			
Nef G2A	+	8	20
Nef $(Pxx)_4$A	–	14	80
Nef T80A	+/–	34	87

Figure 1
HIV-1 Virion Structure and Genomic Organization

Schematic diagram of the structure of HIV-1 showing a cone-shaped core in a spherical envelope. The complex HIV-1 genome is also depicted, possessing at least six additional genes (*nef*, *tat*, *rev*, *vif*, *vpu*, and *vpr*) in addition to the three genes (*gag*, *pol*, and *env*) found in all replication competent retroviruses. (Figure courtesy of Dr. Romas Geleziunas)

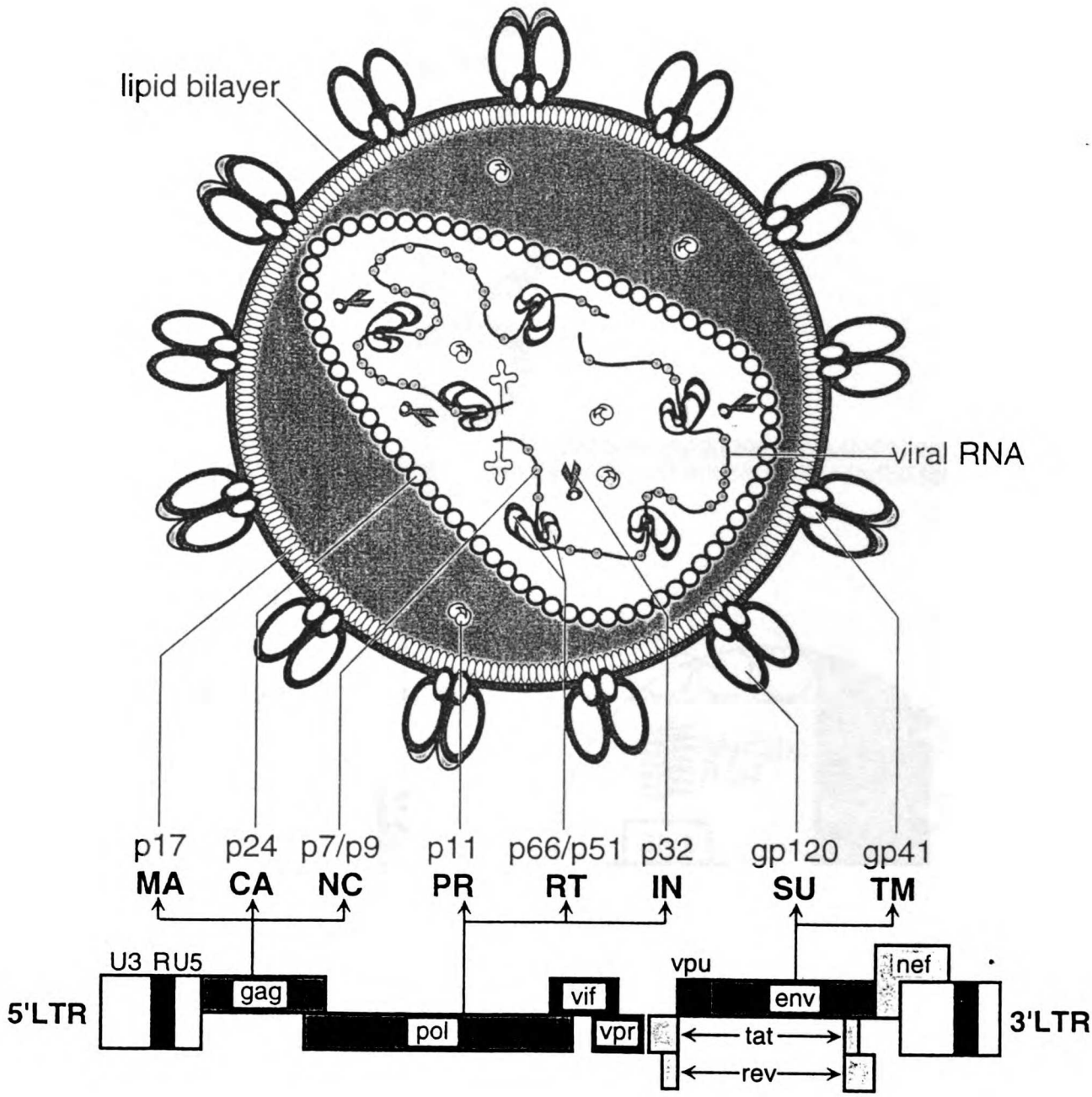

Figure 2
The HIV-1 Receptor: CD4-p56^{lck} Complex

Schematic diagram of the CD4-p56^{lck} complex. Cysteine residues located in the membrane proximal region of CD4 interact with cysteine residues located in the unique region of the Src family tyrosine kinase p56^{lck}.

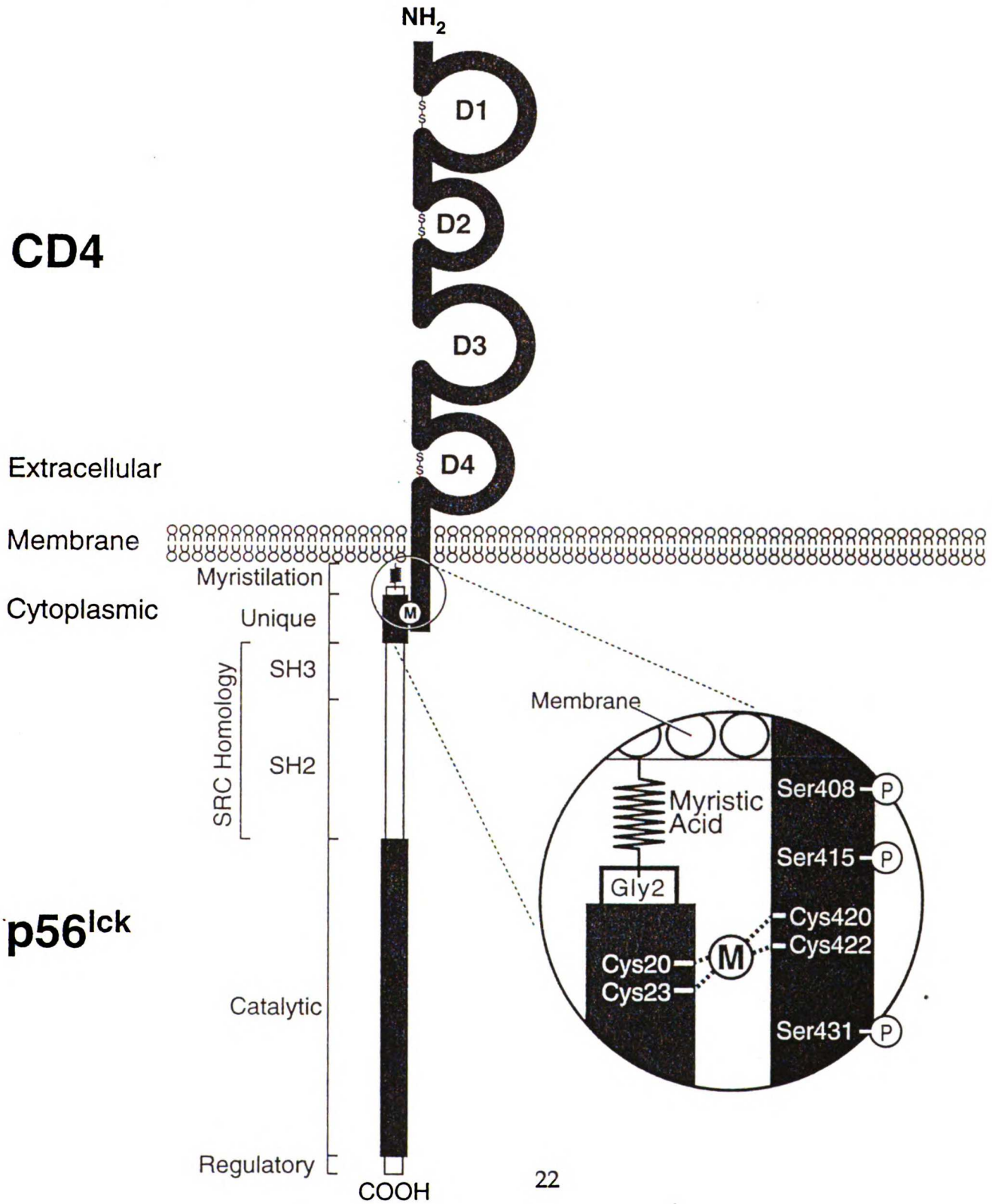

Figure 3
Yeast Two-Hybrid Assay of Protein-Protein Interaction

Diagram of the yeast two-hybrid assay as described by Fields and Song (17). As shown on the top, Protein 1 is fused to the GAL4 DNA binding domain and Protein 2 to the GAL4 activation domain. If the proteins fail to interact, then there is no transcriptional activation of the downstream reporter gene. If the proteins do interact, as shown on the bottom, then the GAL4 factor will be reconstituted, driving transcription of the reporter gene.

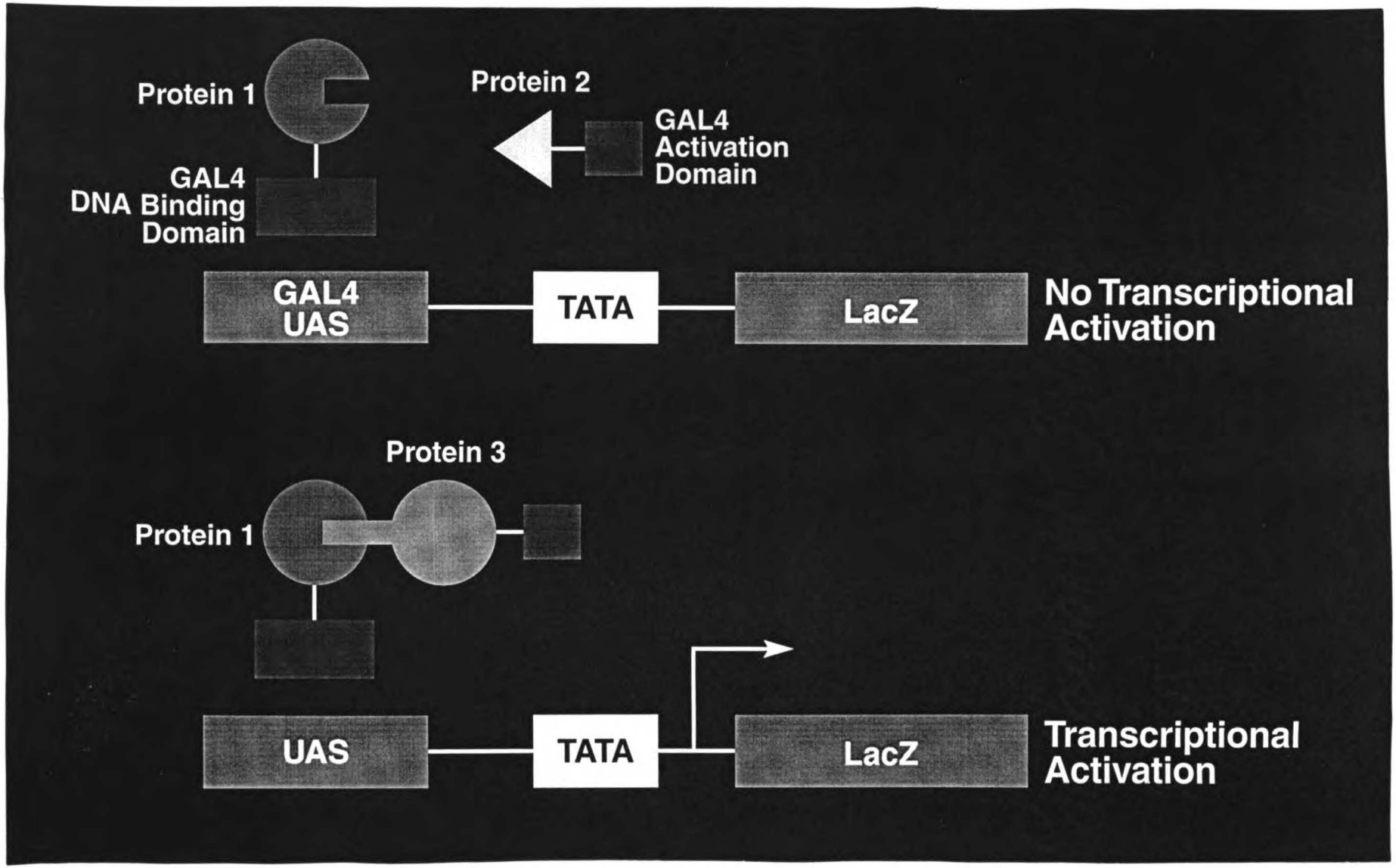

Figure 4

The pGBT9 vector contains the GAL4 DNA binding domain fused to a *trp* marker while the pGAD424 vector contains the GAL4 activation domain fused to a *leu* marker. The HF7c yeast strain was used for library screening and contains two reporter genes, namely, *LacZ* and *His3*.

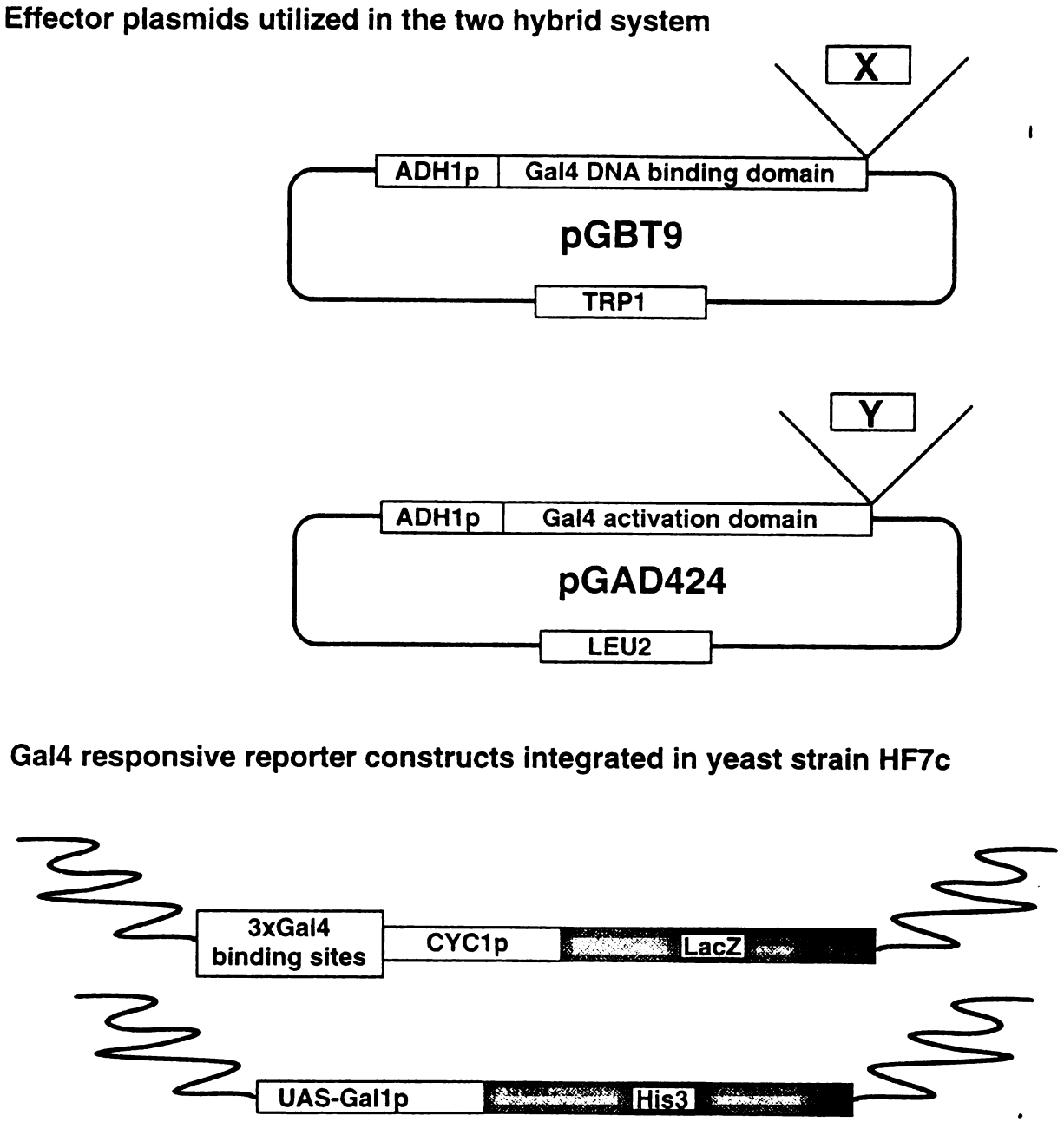

Figure 5
HeLa cDNA Library Screen Using a Nef-Gal4 DNA Binding Domain Fusion Protein (pGBNef)

Flowchart of the HeLa cDNA library screen. 1.7 million Trp+Leu+ yeast transformants representing approximately 25% of the entire cDNA library were screened, resulting in 18 His+LacZ+ clones. The clones were isolated and re-assayed and then tested with a series of controls. The seven remaining clones were sequenced and found to resolve into three different groups of Nef-associating proteins.

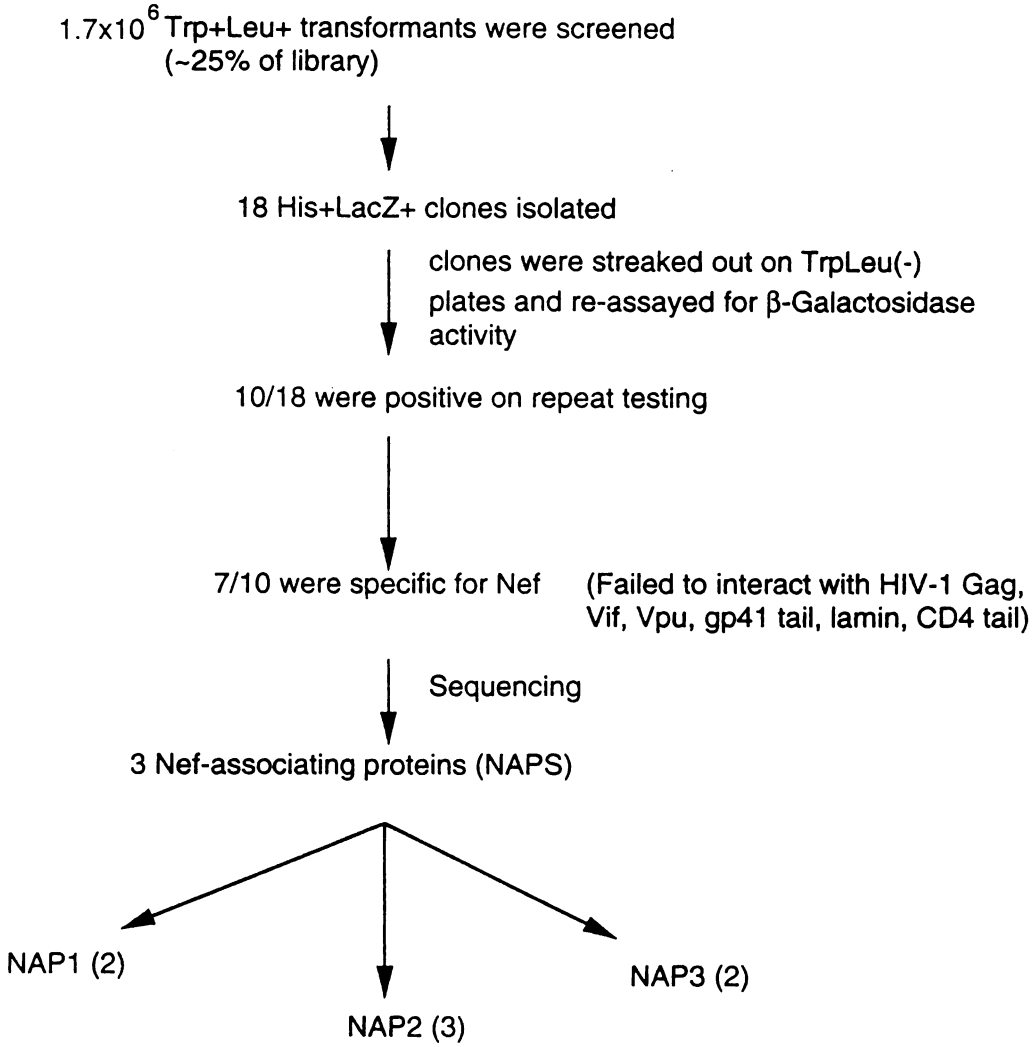

Figure 6
Nef and NAP Interactions

Filters obtained from co-transfomation of yeast with Nef and NAPs 1, 2, and 3. The top plates have undergone a blue color change after addition of the X-gal substrate, demonstrating an interaction between Nef and each NAP. The bottom plate shows Nef transformed with a control vector which remains white after addition of the substrate.

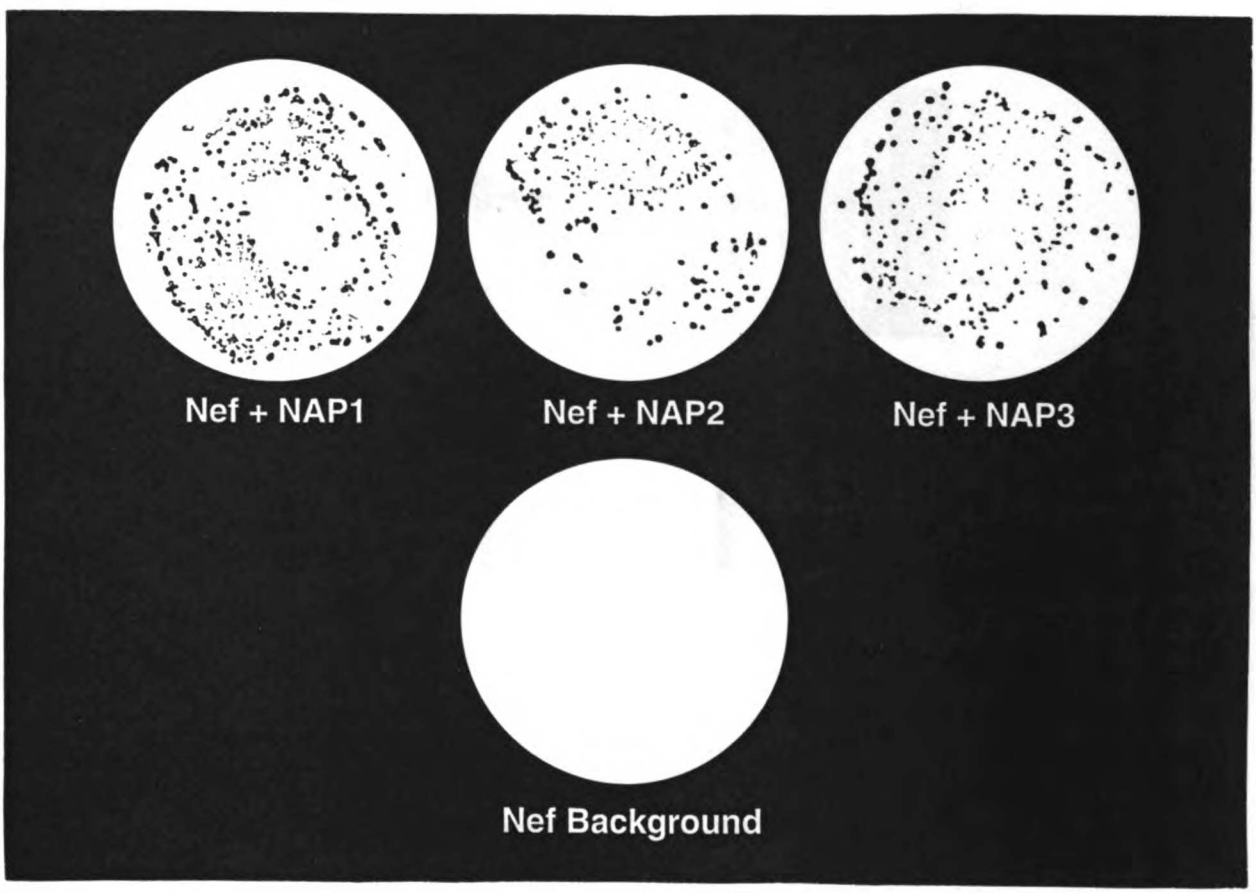

Figure 7
NAP mRNA Species and Tissue Distribution

Northern blot analyses was performed using nitrocellulose filters containing polyA mRNA from various human tissues. cDNA from NAPs 1,2, and 3 were radiolabeled with ^{32}P and used as probes. As shown in this figure, the NAPs were found to be expressed in all tissues tested. However, the patterns of distribution differed, i.e. both NAPs 1 and 3 were most highly expressed in skeletal muscle while NAP2 was most highly expressed in skeletal muscle and spleen. mRNA sizes obtained for NAPs 1,2, and 3 are listed in Table 1.

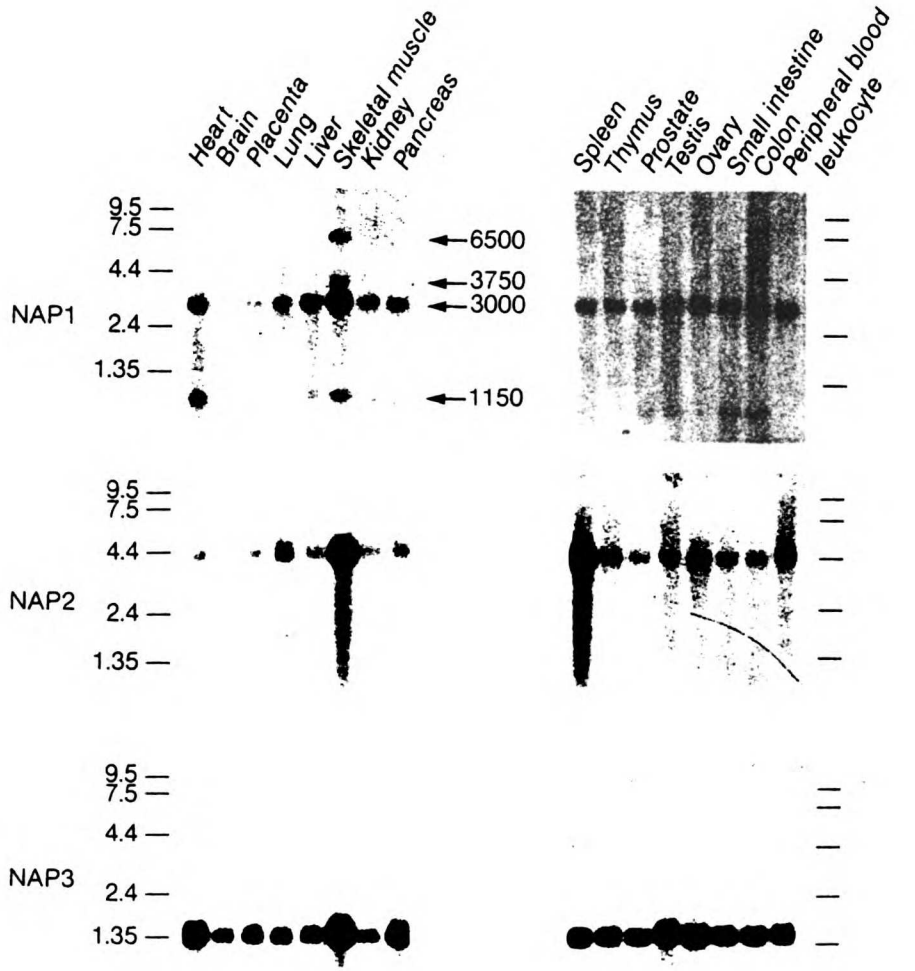

Figure 8
NAP2 Interacts with Both Nef and $p56^{lck}$

Filters obtained from the co-transformation of NAP2 with either $p56^{lck}$ or CD4. The top row of plates demonstrates interactions between both NAP2 and Nef and also between NAP2 and $p56^{lck}$. NAP2 failed to interact with CD4. The bottom row of plates shows Nef, CD4 and $p56^{lck}$ co-transformed with control vectors, with $p56^{lck}$ exhibiting a low level of background transcriptional activity.

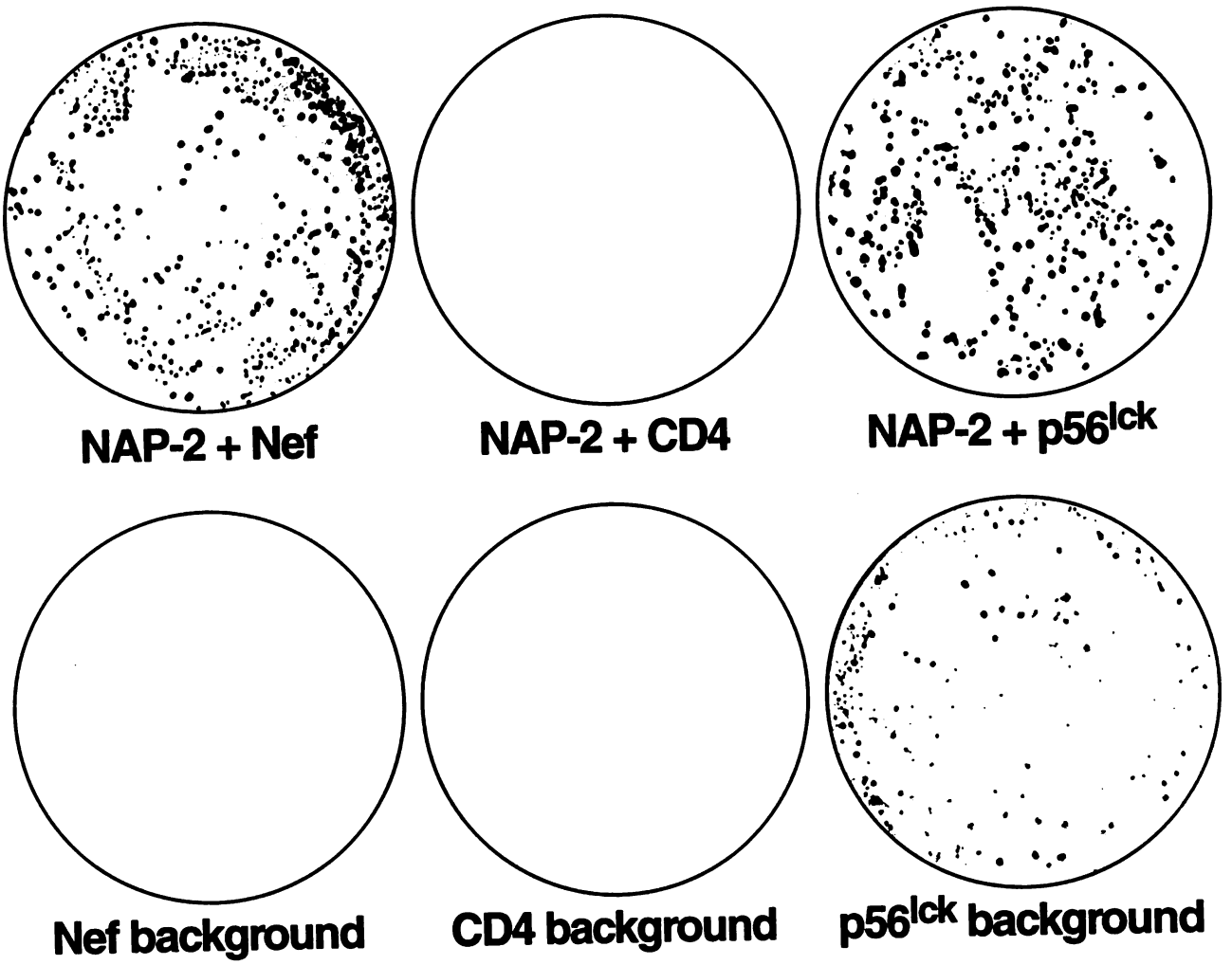

Figure 9A
Deletion Mutant Analysis of NAP2

Chart showing results of co-transformation of deletion mutants of NAP2 with Nef, $p56^{lck}$, and NAP3. N30 refers to a deletion mutant that removes 30 aa from the amino terminus of NAP2, N60 refers to a deletion of 60aa, and N90 refers to a deletion of 90aa. C90 refers to a deletion of 90aa from the carboxy terminus of NAP2, C60 refers to a deletion of 60aa and NAP2 refers to the full length NAP2 clone. From Western blot analysis, it was found that the C30 mutant was not expressed (N.E.) The + symbol indicates the ability to interact, suggesting that the deleted region is dispensable for binding. The - symbol indicates loss of ability to interact, suggesting that the deleted region is critical for binding.

	N30	N60	N90	C90	C60	C30	NAP2
Nef	+	-	-	+	+	N.E.	+
p56lck	+	-	-	+	+	N.E.	+
NAP3	-	-	-	-	+	N.E.	+

Figure 9B
Deletion Mutant Analysis of NAP2

Summary of deletion mutant data show in Figure 9A.

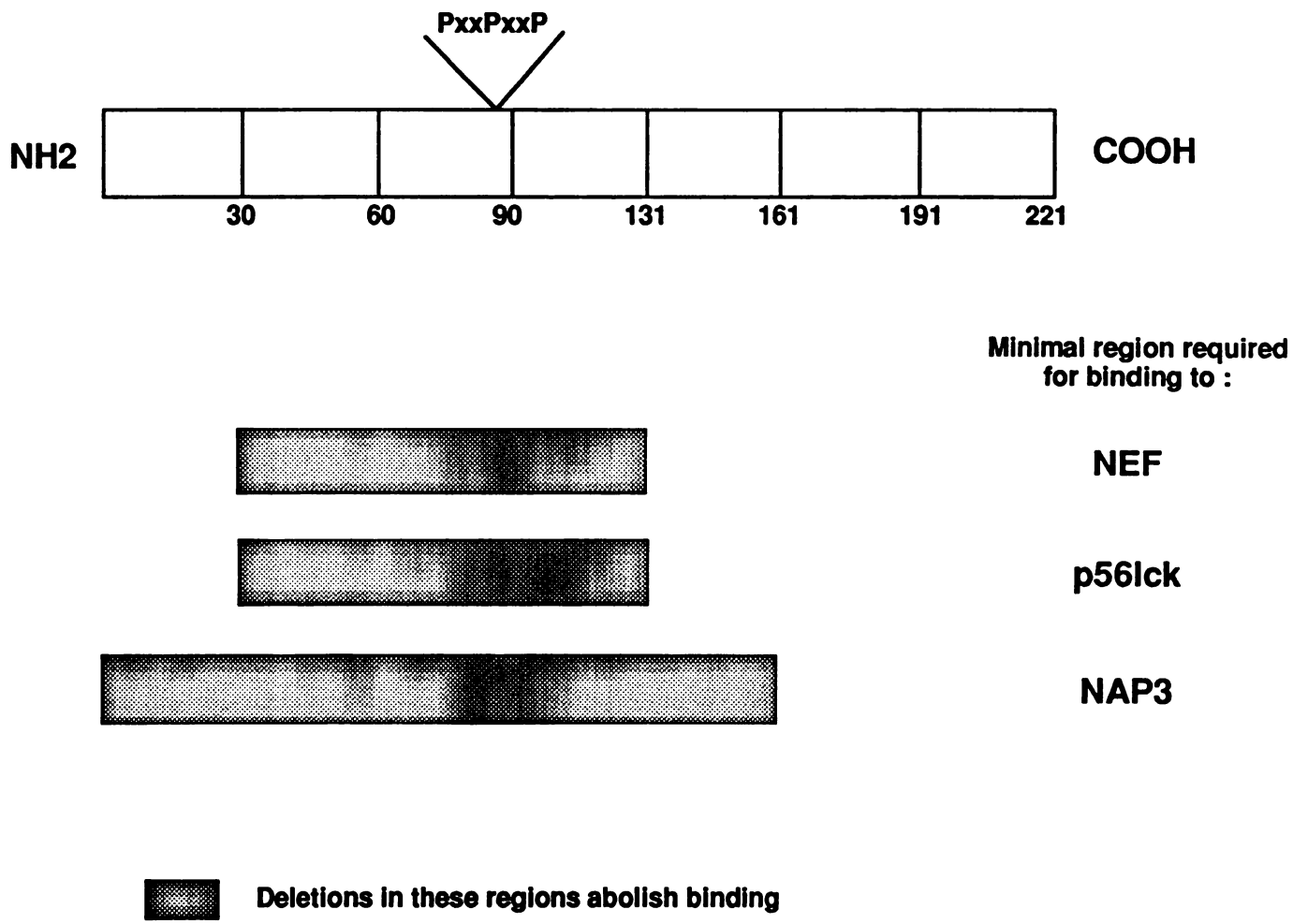

Figure 10
Model 1: Distinct NAP2 Binding Sites

In this first model, NAP2 has distinct binding sites for both Nef and $p56^{lck}$ and serves as a cellular bridge to link Nef to $p56^{lck}$. Removal of $p56^{lck}$ from the cytoplasmic tail of CD4 then allows CD4 to become internalized.

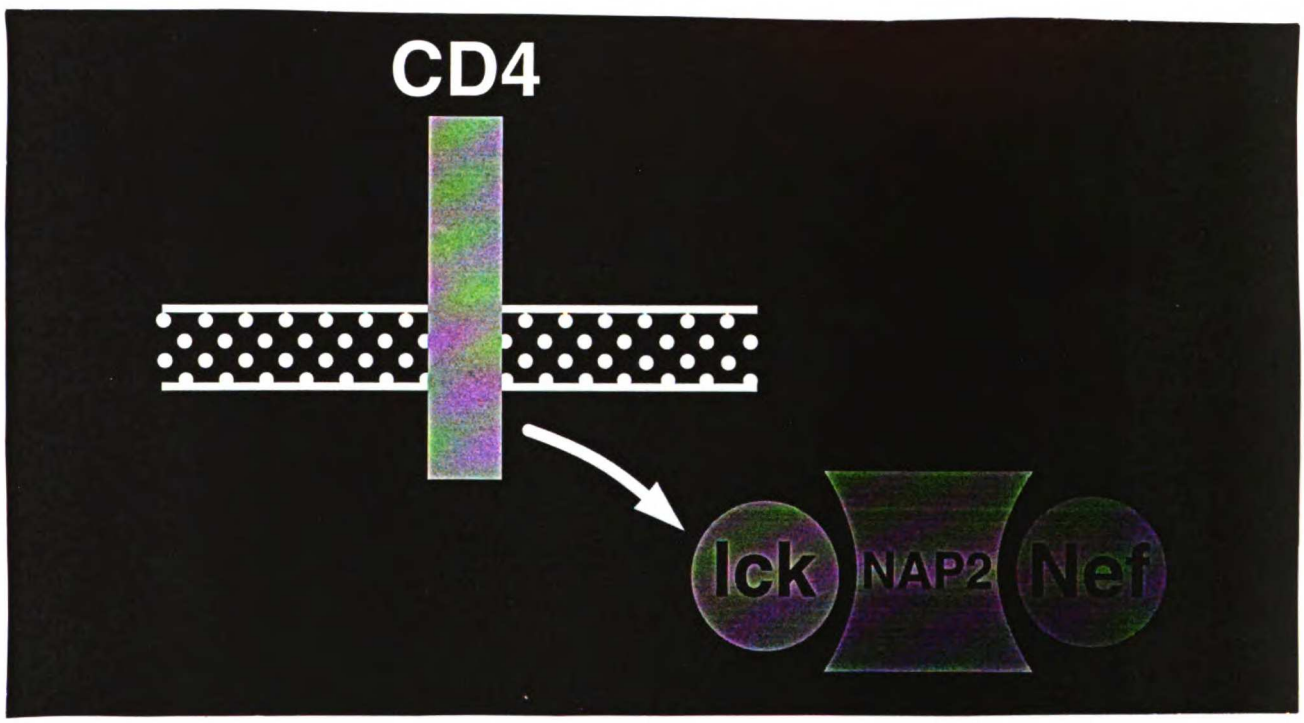

Figure 11
Model 2: Overlapping NAP2 Binding Sites

In this second model, both $p56^{lck}$ and Nef bind to the same region of NAP2 in a competitive manner. In the absence of Nef, as shown in the top portion of the diagram, NAP2 stabilizes the $p56^{lck}$-CD4 complex. In the presence of Nef, as shown in the bottom portion of the diagram, Nef competitively binds NAP2 away from $p56^{lck}$, resulting in its dissocation away from the cytoplasmic tail of CD4. CD4 is then endocytosed.

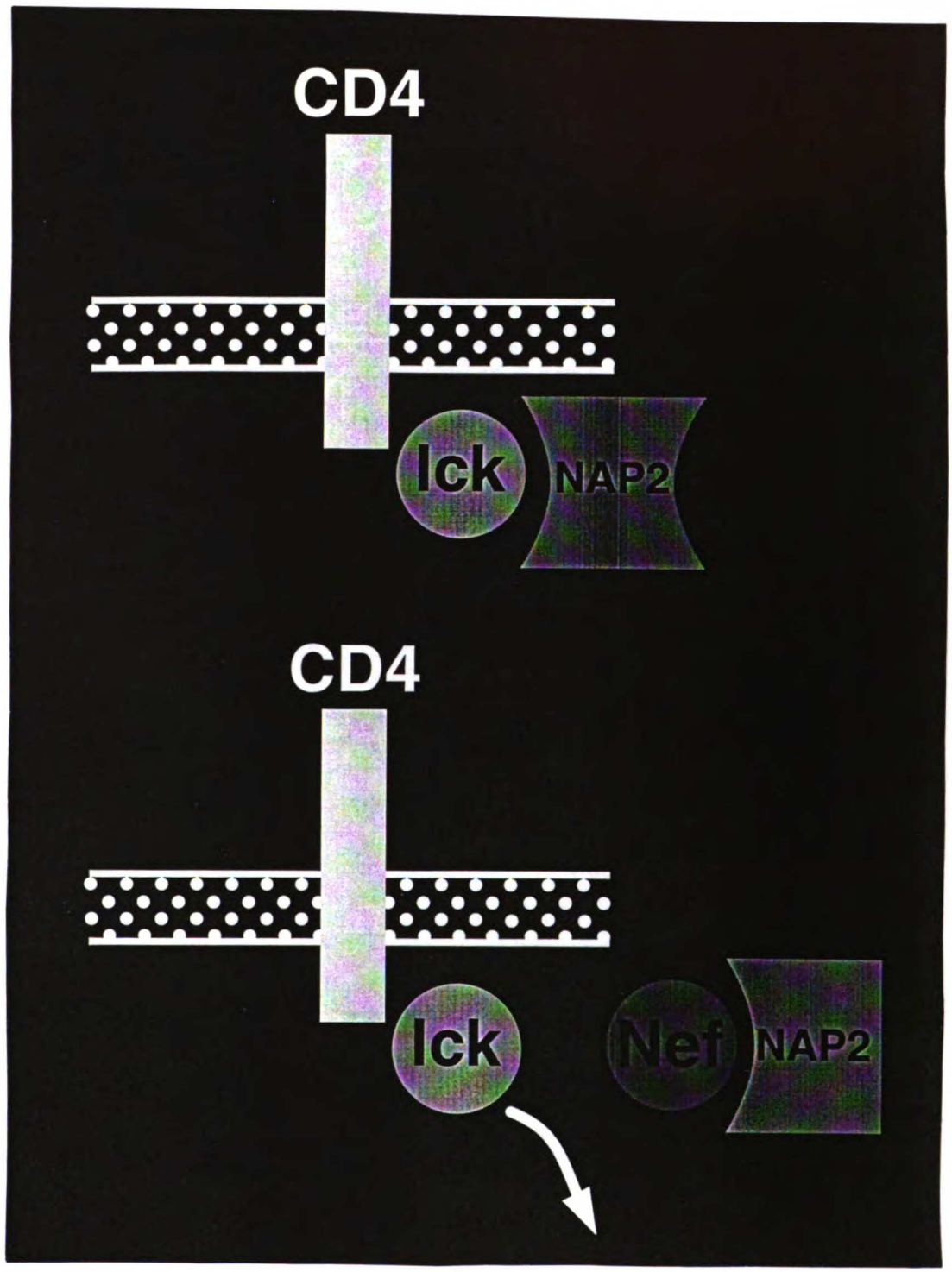

Figure 12
NAP2 Binds Directly to the SH3 Domain of $p56^{lck}$

Schematic diagram showing NAP2 binding directly to the SH3 domain of $p56^{lck}$. Note the PxxPxxP motif in the SH3 binding region of NAP2.